UNIVERSITY OF OKLAHOMA

GRADUATE COLLEGE

HEURISTIC APPROACH TO NETWORK RECOVERY

A THESIS

SUBMITTED TO THE GRADUATE FACULTY

in partial fulfillment of the requirements for the

Degree of

MASTER OF SCIENCE

By

YANBIN CHANG
Norman, Oklahoma
2018

HEURISTIC APPROACH TO NETWORK RECOVERY

A THESIS APPROVED FOR THE
SCHOOL OF INDUSTRIAL AND SYSTEMS ENGINEERING

BY

_____
Dr. Charles Nicholson, Chair

_____
Dr. Janet Allen

_____
Dr. Kash Barker

Acknowledgements

I would first like to thank my thesis advisor Dr. Nicholson. The door to Prof. Nicholson was always open whenever I ran into a trouble spot or had a question about my research or writing. He has taught me more than I could ever give him credit for here. He has shown me, by his example, what a good researcher should be.

I would also like to acknowledge my thesis committee members, Dr. Allen and Dr. Barker, and I am gratefully indebted to their invaluable comments on this thesis.

Finally, I must express my very profound gratitude to my parents for providing me with unfailing support and continuous encouragement.

Table of Contents

List of Tables

List of Figures

Abstract

This study addresses optimization modeling for recovery of a transportation system after a major disaster. In particular, a novel metric based on the shape of the recovery curve is introduced as the objective to minimize. This metric is computed as the distance from the pre-disaster system performance at a time immediately before disruption to the two-dimensional location of the centroid point of the area beneath the recovery curve. The recovery trajectories derived from optimization models with this new metric are considered along with two other recovery goals from literature, i.e., minimizing the total recovery time and minimizing the skew of the recovery trajectory. A genetic algorithm is implemented to search for optimal restoration schedules under each objective and empirical analysis is used to evaluate the corresponding quality of the solutions. Additionally, a particle swarm optimization algorithm is employed as an alternative metaheuristic and the quality of the recovery schedules, as well as the observed computational efficiency is analyzed.

Chapter 1: Introduction and Background

Modern society is profoundly dependent on various infrastructure networks, including electric power, transportation, water supply, sewage handling, and communication and financial systems. To minimize the costs, infrastructure systems are frequently designed to work close to their capability with small margins of reserve capacity and little redundancy (Mattsson and Jenelius 2015). This renders them vulnerable to numerous incidents, such as technical failure, earthquake, extreme storm, flood, nuclear leak and intentional attack. In this paper, we focus on one vital infrastructure network — the road system. The transportation systems play an essential part in supporting the economic and social prosperity of a community. Society is not only dependent on the roadway system for daily commuting, business operation, and supply chain logistics, but also for first-responder, hospital and other critical care accessibility during disasters. Additionally, a functional transportation system is a key to the effective recovery of other infrastructure systems after a disruption, since they provide access for repair crews and equipment to be dispersed throughout the community as needed. Large-scale hazards can impact many roads and bridges in a transportation system. The loss that comes from this damage may be distinguished into two classes: initial direct loss and indirect loss (Zhang et al. 2017). *Direct loss* is the impact due to the immediate damage effects of the catastrophe. For instance, the direct damage would include the physical damage caused by high-velocity winds, flooding, or earthquake, etc. *Indirect losses* are the following or secondary outcomes of the preliminary disruption, such as taxes and revenue losses because of commercial enterprise interruption. The subsequent indirect loss may be equal to or greater even

than the initial direct loss. For example, the initial direct losses in the 2010 Haiti earthquake represents less than half of the total economic loss to-date (UNISDR, 2011). Resilience modeling has become a critical methodology representing a new way to recognize and manage system vulnerabilities and for analyzing the recovery problem of complex networks. Resilience has been explored in the literature in many areas of engineering (Filippini and Silva 2014; Cutter et al. 2010). A well-accepted definition of infrastructure network resilience is provided by Bruneau et al. (2003) as shown in Figure 1, where resilience is characterized by four dimensions: *robustness*, the capacity to minimize the direct loss after disruption; *redundancy*, the degree of which components and elements are substitutable in a system; *resourcefulness*, the ability of a system to provide appropriate measures in order to overcome the damage; *rapidity*, the speed at which the system can return to a specified level of functionality. Various techniques to measure resilience can be found in Bruneau et al. (2003), Chang and Shinozuka (2004), Barker et al. (2013), Cimellaro et al. (2006, 2010), Tamvakis and Xenidis (2013), and Sterbenz et al. (2013). Several studies have been focused on specific engineering areas, such as transportation systems (Zhang and Hooks 2015; Zhang and Wang 2016), supply chains (Ponomarov and Holcomb 2009; Raj et al. 2015), airline system (Wang and Ip 2009), power grids (Shinozuka et al. 2003; Nan and Sansavini 2017) and water distribution systems (Odan et al. 2015; Zhang et al. 2017)

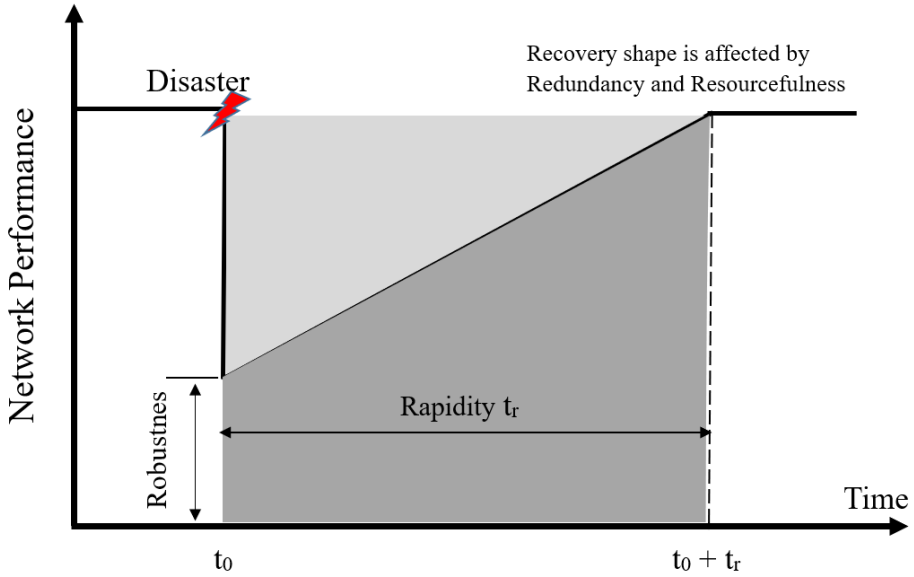

Figure 1. Illustration of Resilience Definition (Bruneau et al. 2003)

Shinozuka et al. (2000) presented a statistical analysis of the structural fragility curve in a bridge system. Later, based on an examination of the seismic performance of the Los Angeles Department of Water and Power (LADWP) system after the Northridge earthquake, Shinozuka et al. (2003) used the fragility information of electrical power equipment to simulate the recovery process after earthquakes. Two dimensions of resilience, robustness and rapidity, are used to describe restoration process modeling. Çağnan et al. (2004) built a simulation model of a multi-lifeline restoration process in the LADWP electric power system. The advantage of their model is the ability to change the model flexibility in comparing the different restoration strategies by identifying restoration curves and simulating the relatively realistic model.

Miles and Chang (2004) developed a comprehensive conceptual model of recovery and indicated the necessity to consider realistic factors during the recovery process. Their model establishes the essential relationships among the community's lifeline networks, household's businesses and neighborhoods. Davidson and Çağnan

(2004) discussed a post-earthquake recovery model for an electric power network. The model was built to reduce the restoration time and identify ways to enhance the systems' performance in the future disaster. A study by Xu et al. (2006) produced a stochastic integer model to select the recovery plan to optimize the post-disaster restoration of the electric power network. Their model's objective is to minimize the triangular area above the recovery curve, i.e., the "resilience triangle" from Bruneau et al. (2003).

Frangopol and Bocchini (2011) developed a framework for evaluating the performance of road transportation systems considering the restoration process regarding resilience and economic cost. The performance of the networks is measured by the total travel time distance. In Bocchini and Frangopol (2012), the authors added two other objectives: the minimization of recovery time to satisfy a particular level of system functionality and the minimization of the total cost of restoration. Karamlou and Bocchini (2014) presented a methodology for scheduling the recovery sequence of road networks based on multi-objective combinatorial optimization using Genetic Algorithms. Their objective was to maximize the resilience and minimize the time required to connect the critical nodes of the network. More recently, Karamlou and Bocchini (2016) proposed an optimization technique called "Algorithm with Multiple-Input Genetic Operators" for independent scheduling tasks considering resource and time constraints.

Numerous resilience analysis metrics have been developed and implemented for evaluating the post-disaster restoration process including the total travel time and distance, recovery time, financial loss, and the resilience triangle. Zhang et al. (2017) proposed a novel technique to analyze the efficiency of recovery schedule, based on the shape of the area below the restoration trajectory (resilience trapezoid). The authors gave an example as

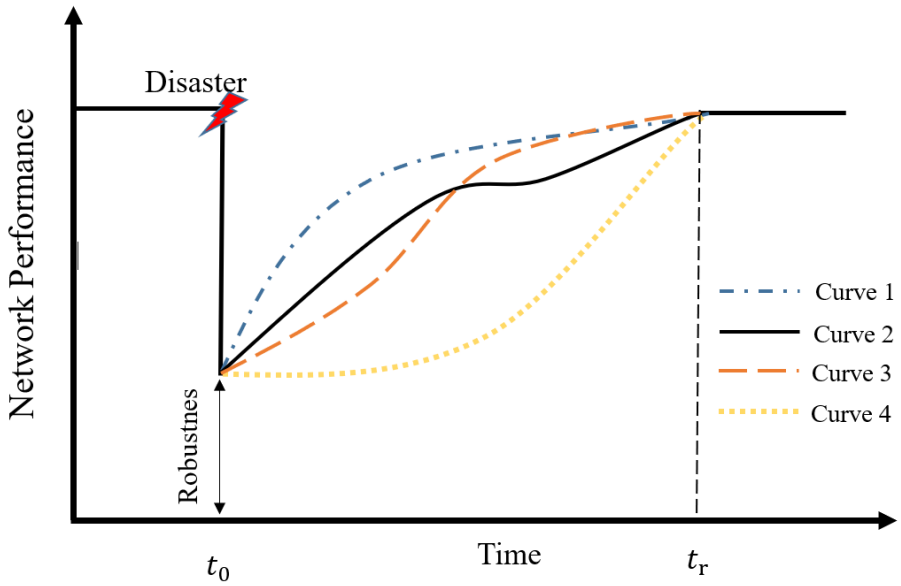

Figure 2. Different Recovery Trajectories

showed in Figure 2 in which the four restoration trajectories have an equal total recovery time. Assuming equal quantity of community rebuilding funds, curve 1 represents the most desirable recovery plan, whereas curve 4 is the least favorable among the options. Furthermore, curve 2 is arguably superior to both curves 3 and 4 since its early-period restoration outperforms both. Rapid restoration in the early portion of the recovery horizon reduces the time at which the community must endure low levels of functionality. This performance in the early segment of rebuilding process could also aid the quick recovery of other critical infrastructures whose service

effectiveness notably rely on the capacity of transportation systems (e.g., emergency medical system, rescue operations following disaster events). To quantify the novel recovery process trajectory, Zhang et al. (2017) introduced a new metric, the *skew of the recovery trajectory* (SRT), for measuring the relative performances of various network recovery schedules. The SRT metric will be detailed in Chapter 3.

To evaluate the efficiency of metrics, we build a stochastic restoration scheduling model. Several properties are set to be random in this model – in particular, we randomize the necessary restoration time for each road and the location of disaster center. We introduce a novel method for evaluating the recovery trajectory based on an enhancement of the SRT approach. The new metric is the *centroid of the recovery trajectory distance* (CRTd). A Genetic Algorithm (GA) is implemented to search for near-optimal schedules of the problem under various objectives. The three objectives are the minimization of TRT, SRT, and CRTd, respectively. The recovery schedules determined by minimizing these three metrics will be compared. At last, considering the lengthy computation time of GA, we will rebuild the model by Particle swarm optimization algorithm (PSO), then compare the performance of both algorithms by statistical analysis.

The paper is organized as follows. In the following chapter, we propose the metric of calculating overall network performance used in this study. In Chapter 3, we define the three metrics for evaluating the efficiency of the recovery schedules, including the novel CRTd metric, and introduce the algorithms we used to build the optimization models. In Chapter 4, we empirically analyze network recovery trajectories based on the different objectives. Additionally, we compare the performance of two

metaheuristics approaches to identify near-optimal schedules. Chapter 5 concludes the work.

Chapter 2: Performance Metric of Road Network

The effective flow of people, commodities, and other measured items is often used to indicate the performance of networks such as the electricity grid, transportation system, and supply chains. For example, Harris and Ross (1955) first mentioned the maximum flow model in their study of Soviet Union railway traffic. Maximum flow analysis is used to identify the maximum feasible flow through a capacitated, single-source, single-sink flow network (Schrijver 2002). Maximum network flow provides the fundamental metric used in the present work to measure system performance. In particular, if V denotes the set of all vertices in a network, the all pairs max flow problem (APMF) is equal to the sum of the maximum flow from $s \in V$ to $t \in V$, for all (s, t) pairs in $V \times V$, such that $s \neq t$. We use the APMF to indicate the performance level of the transportation network.

There are many methods to compute maximum flow in a network, such as linear programming, the Ford-Fulkerson algorithm (Ford and Fulkerson 1956), the Edmonds-Karp algorithm (Edmonds and Karp 1972) and the Push-relabel algorithm with dynamic trees algorithm (Goldberg and Tarjan 1988). For a large complex network, these methods may take a long time to calculate all pairs max-flow. For example, consider the LP approach. The mathematical formulation is adapted from Wang (2015). Let $G = (V, E)$ denote a network where V is a set of n vertices, and E is a set of m edges. The parameter c_{ij} denotes the capacity of edge $(i, j) \in E$. The decision variable x_{ij} in the LP denotes the flow from node i to node j on edge $(i, j) \in E$. The variable f_{st} denotes the flow from s to t for a given source and sink node pair $(s, t) \in V \times V$. If $s = t$, then f_{st} is equal to 0. An LP all pairs max flow optimization problem is formulated in Equations

(1)-(3):

$$\text{Max } f_{st} \tag{1}$$

$$\text{s.t. } \sum_{(i,j)\in E} x_{ij} - \sum_{(j,i)\in E} x_{ji} = 0,\ \forall\, i \in V\backslash\{s,t\} \tag{2}$$

$$0 \le x_{ij} \le c_{ij} \tag{3}$$

Equation (1) is the objective function. Equation (2) reflects the flow-balance constraints in the network. Note that the flow-balance constraints are required for all nodes in the network, except for the source and sink nodes. Equation (3) ensures there is no negative or overloaded flow in the network. Let f_{st}^* denote the maximum flow from the solution to the APMF formulation described in Equations (1)-(3). The all pairs maximum flow can be calculated, $\varphi_{all} = \sum_{(s,t)\in V} f_{st}^*\ \forall\, s \neq t$. For a network with n nodes, the APMF optimization problem can be solved after $n\ (n-1)$ times iterations: once for each distinct node pair. Note that, in the bi-directional and symmetric graphs, we know that $f_{st}^* = f_{ts}^*$. Then, the quantity of all pairs max flow problems to be calculated is then $\frac{n(n-1)}{2}$. Practically speaking, the computation time may be very long due to the size of the network, even though we can reduce the total calculations by half. The time complexity of linear programming is $O(mn^2)$; for Ford-Fulkerson algorithm is $O(mK)$, where K is defined as the maximum pairwise connectivity between any pair of vertices in the graph; for the Edmonds-Karp algorithm, the computational complexity is $O(m^2 n)$; and for the Push-relabel algorithm with dynamic trees algorithm it is $O(mn \log_m n^2)$ (Edmonds and Karp 1972; Goldberg and Tsioutsiouliklis 2001). The truth is, if we use the methods mentioned above, even a single calculation of φ_{all} in a complex network needs a long computing time, while we need to measure the

φ_{all} value during the whole process of recovery schedule searching. However, all above algorithms are not ideal choice of the problem take into consideration the application of selecting k out of m edges for restoration after disruption, where the set of k edges is sequentially repaired, a complete evaluation would require $\binom{m}{k}$ computations of φ_{all}.

The Gomory-Hu trees algorithm uses minimum $s-t$ cuts for computing all node pairs maximum flow (Hariharan et al. 2007). Gomory and Hu (1961) first confirmed that the edge connectivities of all pairs of vertices in an undirected graph could be evaluated using $n-1$ max-flow computations (instead of the naïve $\binom{n}{2}$ computations). Their algorithm computes a weighted cut tree T called the Gomory-Hu tree, on V, with the property that the edge connectivity between any two vertices s and t in V precisely equals the weight of the minimum weight edge on the unique $s-t$ path in T. Furthermore, the partition of the vertices produced by removing this edge from T is a minimum $s-t$ cut in the graph. The time complexity of Gomory-Hu tree algorithm on undirected weighted graphs is $O(mn)$. Hence we pick Gomory-Hu tree algorithm to compute the performance of road network. In this study, a transportation network is wholly recovered if the network performance φ_{all} returns to its pre-disruption value.

Chapter 3: Optimization of Network Restoration Scheduling

3.1 Evaluation Metrics for Network Recovery Plan

In this chapter, three evaluation metrics for the post-disaster recovery schedule trajectory are described. The first metric is the *total recovery time* (TRT), starting from the beginning of restoration process and ending at the time when the network is fully recovered, i.e., the time when all edges are restored to their full capacity. As shown previously, Zhang et al. (2017) demonstrated that the TRT is not sufficient to evaluate a recovery plan. For instance, Figure 3 demonstrates two restoration schedules with nearly equal TRT (the performance of the network is measured by APMF). The initial performance and immediately disrupted performance are indicated in Figure 3 as p_0 and p_d, respectively. It is apparent that while recovery curves 1 and 2 share similar total restoration time, curve 1 is superior to curve 2 due to the quick early recovery which will minimize cumulative losses throughout the restoration horizon.

Consequently, another metric which used to compare the efficiency of network restoration strategies is the *skew of recovery trajectory* (SRT). This metric is equal to the centroid coordinate on time-axis of the region beneath the trajectory, i.e., from t_0 to t_l (Zhang et al., 2017). S_1 and S_2 in Figure 3 denote the SRT values related to curve 1 and 2, respectively. While the TRT is very close between two curves in Figure 3, clearly, $S_1 < S_2$.

The third metric is a novel enhancement of the SRT which we introduce in this work. The metric, *centroid of recovery trajectory distance* (CRTd), is demonstrated in Figure 4, and represents the distance between the centroid point

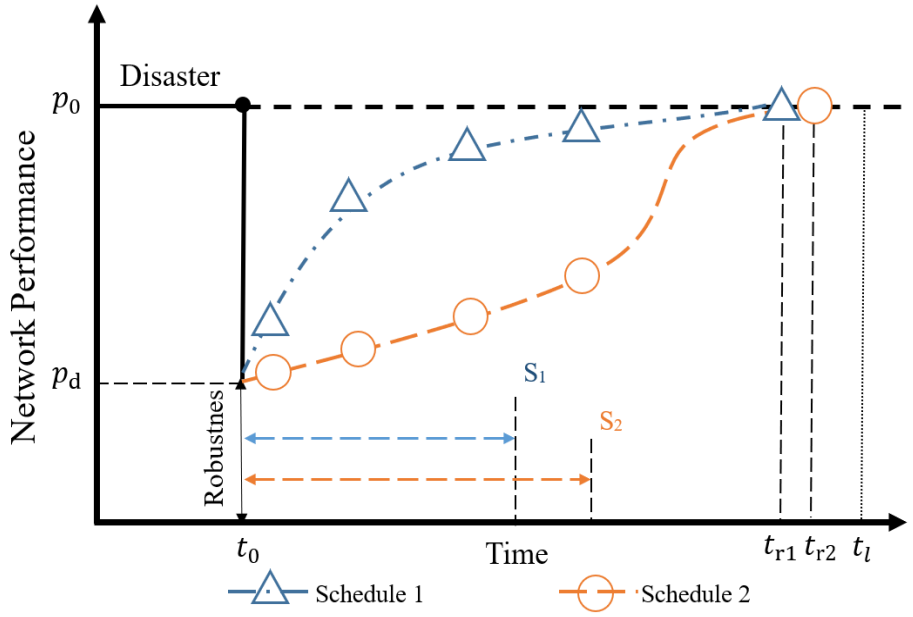

Figure 3. Skew of Recovery Trajectory

of the trapezoid area beneath the recovery trajectory and the initial point C_0 representing the pre-disaster system performance. In Figure 4, the centroid point associated with schedule 1 and 2 are marked as C_1 and C_2, respectively. We hypothesize that by introducing the system performance dimension into the skew metric, optimizing with respect to the novel CRTd measure will produce distinct, and superior, recovery trajectories.

In this thesis, $T = \{t_0, t_1, t_2 \dots t_r\}$ are the time points during the restoration process. Each point means that there is a changing of network performance value occurring. Let $E = \{1, 2, 3 \dots m\}$ denote the set of roads in network, and let q_e denote the initial capacity of road e before a disaster occurs. The value q_e^t denotes the capacity of road $e \in E$ at time point $t \in T$ calculated by,

$$q_e^t = q_e \cdot q_{ed}^t \tag{4}$$

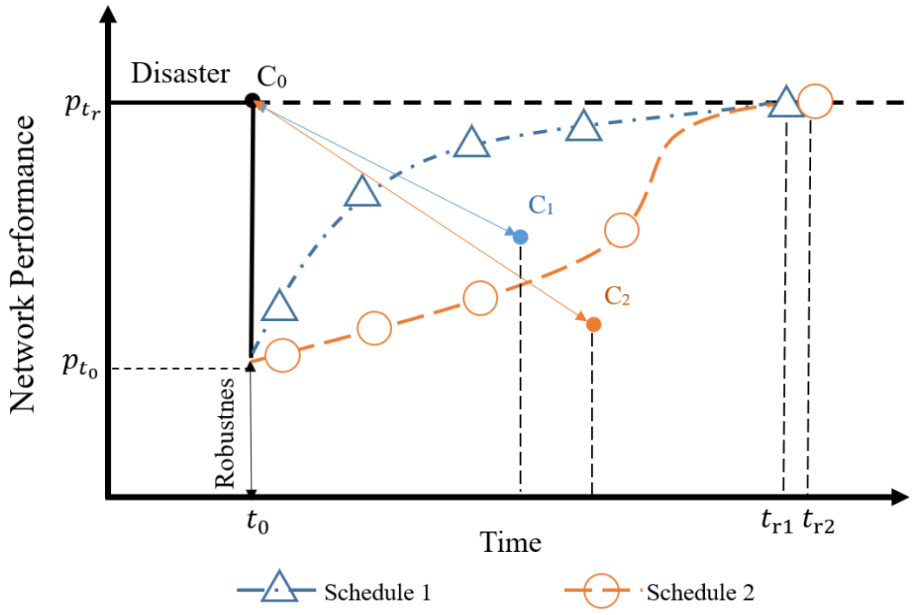

Figure 4. Centroid of Recovery Trajectory

where q_{ed}^t is the damage index of road e at time t, defined on a five point scale from 0 to 4. If $q_{ed}^t = 0$, there is no damage and the associated roadway is at full capacity. For q_{ed}^t values 1 to 4, the disruption corresponds to roadway capacities at 80%, 50%, 20%, and 0% of the original service level q_e, respectively. Let $p(t)$ denote the APMF network performance at time t based on the dynamic road capacities, i.e.,

$$p(t) = \varphi_{all}\,(q_1^t, q_2^t \ldots q_m^t) \tag{5}$$

Let the set of damaged road segments be denoted by $\mathcal{E} \subseteq E$. Assume $|\mathcal{E}| = k \leq m$. Without loss of generality, let the set $\mathcal{E} = \{1, 2 \ldots k\}$. Let $\mathbb{x} = \{x_1, x_2, x_3 \ldots x_k\}$ denote the start times for initiating repair on the damaged roads. Additionally, let $D_{\mathcal{E}}$ denote the necessary restoration times for each of the damaged road in $\mathcal{E}$. We assume restoration actions are non-preemptive. That is, once a roadway restoration action is initiated, it must be finished before the associated maintenance crew moves to repair another roadway segment. A disrupted road capacity remains at the initial damage level

q_{ed}^{t} until its restoration process is completed. The recovery TRT of schedule $\mathbb{x}$ is denoted as $t_r(\mathbb{x})$, and defined in Equation (6),

$$t_r(\mathbb{x}) = \underset{e\in\mathcal{E}}{Max}\,(x_e + D_e) - t_0 \tag{6}$$

Let t_l denote a point in time which exceeds all conservative estimates for a system's TRT. This value is used as a shared reference time for calculating SRT of distinct recovery strategies. The SRT corresponding to schedule $\mathbb{x}$, $s(\mathbb{x})$ is:

$$s(\mathbb{x}) = \frac{\int_{t_0}^{t_l} p(t)\cdot(t-t_0)\,dt}{\int_{t_0}^{t_l} p(t)dt} \tag{7}$$

Let Δt denote the time between sequential time points when the network performance is changed. Also, we set the t_0 as 0, means that the beginning time of recovery process is 0. Then, the $s(\mathbb{x})$ can be approximated by

$$s(\mathbb{x}) \approx \frac{\sum_{i=0}^{l} t_i p(t_i)\,\Delta t}{\sum_{i=0}^{l} p(t_i)\,\Delta t} \tag{8}$$

The calculation of CRTd needs two coordinate points: the initial point C_0 (as shown in Figure 4) and the centroid point. Let $(c(\mathbb{x}_t), c(\mathbb{x}_p))$ denote the two dimeinsonal coordinate of centroid point of the resilience trapezoid with respect to the time-axis and performance-axis, respectively. Similarly to the calculating of $s(\mathbb{x})$, the $c(\mathbb{x}_t)$ and $c(\mathbb{x}_p)$ associated with scheduling strategy $\mathbb{x}$ can be approximated by Equations (8) and (9):

$$c(\mathbb{x}_t) = \frac{\int_{t_0}^{t_r} P(t)\cdot(t-t_0)dt}{\int_{t_0}^{t_r} P(t)dt} \approx \frac{\sum_{i=0}^{r} t_i P(t_i)\,\Delta t}{\sum_{i=0}^{r} P(t_i)\,\Delta t} \tag{9}$$

$$c(\mathbb{x}_p) = \frac{\int_{p_{t_0}}^{p_{t_r}} [t_{p_{t_r}} - t(p)]\cdot(\mathrm{p}-p_{t_0})dp}{\int_{p_{t_0}}^{p_{\mathrm{tr}}} [t_{p_{t_r}} - t(p)]dp} \approx \frac{\sum_{j=p_{t_0}}^{p_{t_r}} [t_{p_{t_r}} - t(j)]\cdot(p_j - p_{t_0})\Delta p}{\sum_{j=p_{t_0}}^{p_{t_r}} [t_{p_{t_r}} - t(j)]\Delta p} \tag{10}$$

In the Equation (9, 10), t_r set to be the specific total recovery time of each

reconstruction schedule. p_{t_0} is defined as the robustness of network which equals to the network performance at the beginning of reconstruction process, p_{t_r} equals to the initial network performance before the hazard event occurs, also equals to the performance of network when then recovery is finished. Let N_t denote the total number of roads which are under repair at time t. N_{max} is the maximum number of simultaneous repairing roads in the entire network, which is depending on the resources available for the recovery process after the disaster. The optimal recovery sequence for all damaged roads is obtained by minimizing TRT (as defined by Equation (6)) or SRT (as defined by Equation (8)) or CRTd (as defined by Equation (9, 10)). The optimization problems under investigation are summarized in Table 1.

Additionally, we introduce a generic method to evaluate the quality of competing schedules which is not specifically tied to the formulations of the three optimization problems. The measure is based on the concept of the future value of an investment. More specifically, the system performance loss (see the upper left portion in Figure 5), is not necessarily equivalently valued throughout the recovery horizon. That is, the system loss is evaluated as the *future value* of the loss at the time point of the final recovery assuming a rate of return $\theta \geq 0$. This loss function is presented in Equation (11):

$$Loss = \int_{t_0}^{t_r} (p_{t_r} - p_t) \cdot (1+\theta)^{t_r - t}\, dt \qquad (11)$$

Note that, each recovery schedule uses its particular t_r, the recovery processing time, to calculate the loss function. Since we are uncertain about the right value of θ (which is more likely defined by authorities). In our study, we set $\theta = 0.01$; a value

could demonstrate the importance of early-period restoration without exaggerated.

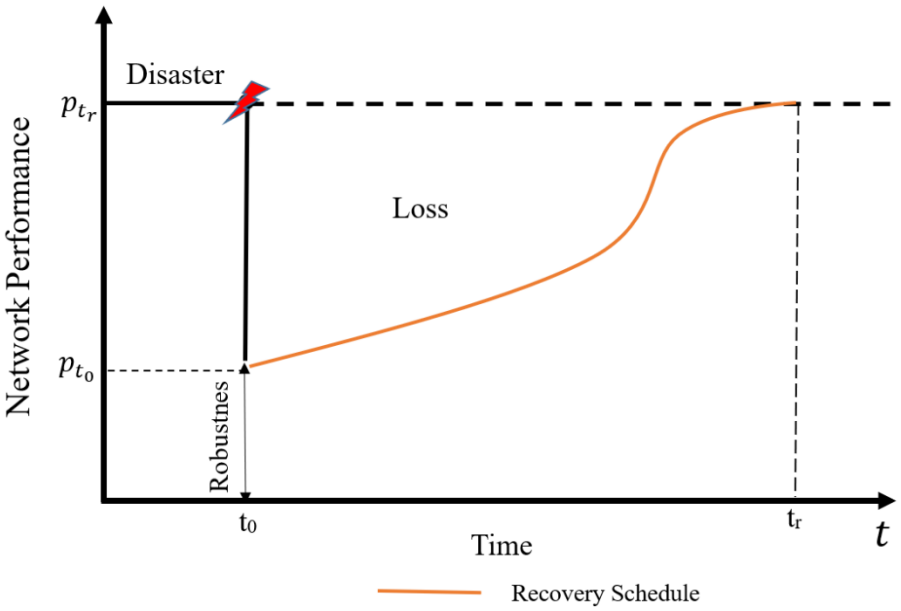

Figure 5. Loss Function

Table 1. Summary of the Optimization Formulation

Description:	Equations:	Eq. No.:
Input Parameters	Network topology: $G = (V, E)$ Damage level of road: $q_{ed}^{t} \in \{0, 1, 2, 3, 4\}\ \forall$ e $\in E$ Road restoration duration: $D_{\mathcal{E}}\ \ \mathcal{E} = 1, 2 \ldots k$	
Decision Variables	$\mathbb{x} = \{x_1, x_2, x_3 \ldots\ x_k\}$	
Global Objective 1 Minimize total recovery time	$\min t_r(\mathbb{x}) = \underset{\mathcal{E} = 1, 2 \ldots k}{Max} (x_{\mathcal{E}} + D_{\mathcal{E}}) - t_0$	(6)
Global Objective 2 Minimize skew	$\min s(\mathbb{x}) = \frac{\sum_{i=0}^{l} t_i P(t_i)\ \Delta t}{\sum_{i=0}^{l} P(t_i)\ \Delta t}$	(8)
Global Objective 3 Minimize centroid distance	$\min \sqrt{[t_0 - c(\mathbb{x}_t)]^2 + [p_{t_r} - c(\mathbb{x}_p)]^2}$	
	$c(\mathbb{x}_t) = \frac{\sum_{i=0}^{r} t_i P(t_i)\ \Delta t}{\sum_{i=0}^{r} P(t_i)\ \Delta t}$	(9)
	$c(\mathbb{x}_p) = \frac{\sum_{j=p_{t_0}}^{p_{t_r}} [t_{p_{t_r}} - t(j)] \cdot (p_j - p_{t_0}) \Delta p}{\sum_{j=p_{t_0}}^{p_{t_r}} [t_{p_{t_r}} - t(j)] \Delta p}$	(10)
Constraint 1 Network performance at time t	$p(t) = \varphi_{all}\ (q_1^t, q_2^t \ldots q_m^t)\ \forall\ t\ \in T$	(5)
Constraint 2 Simultaneous restoration cannot exceed the maximum number	$N_t \leq N_{max}\ \ \forall\ t\ \in T$	
Constraint 3 Complete recovery time	$t_{cr}(x) = x_{\mathcal{E}} + D_{\mathcal{E}}\ \ \mathcal{E} = 1, 2 \ldots k$	
Constraint 4 Variable interval	$x_{\mathcal{E}} \geq 0\ \ \mathcal{E} = 1, 2 \ldots k$	

3.2 Genetic Algorithms and Particle Swarm Optimization Algorithm

The optimization model in this work is similar to the parallel machine scheduling problem, which has been widely studied in past decades and there are no known polynomially bound algorithms for this problem (Weng et al. 2001; Franca et al. 1996; Guinet 1993). However, genetic algorithms (GA) are bio-inspired optimization methods that are commonly used to solve complex scheduling problems (Holland 1975; Goldberg 1989). The input of the GA is a set of solutions called the population of individuals that will be evaluated. As soon as the evaluation of individuals is achieved, parent solutions are selected and a crossover mechanism is implemented to achieve a brand new generation of individuals (offspring). Furthermore, the mutation technique is applied as a way to bring variety into the population. Additionally, the GA flowchart (Figure 6) described by Karamlou and Bocchini (2016) is modified to apply to this project. In this paper, we use the same GA parameters for all models: population size is 40, the mutation rate is 0.2, and the cycle crossover operator is applied. The maximum number of iterations is 10000, and the early termination criterion is 50.

Genetic algorithms often require a long computing time when applied a complicated network. As such we attempt to find a faster approach, the Particle swarm optimization (PSO) was proposed by Kennedy and Eberhart (1995) and is an algorithm inspired by the collective behavior of bird and fish. PSO is one of the latest evolutionary optimization techniques for optimizing continuous nonlinear functions (Kashan and Karimi 2009). The essential PSO flow diagram is depicted in Figure 7. PSO has many similarities to GA: both begin with a randomly generated population of solutions; both employ fitness values to iteratively guide modifications of the population; and both use

stochastic elements to approach to the optimum. However, PSO updates its population of solutions with the two best solutions' (global and local) information, in GA, the individuals are updated by several best solutions. In this paper, we build a swap operator based PSO model which was introduced by Wang et al. (2003). Set population size to be 40, and the alpha and beta swap parameter both equal to 2.05. Two metaheuristic features of PSO and GA are compared in this study: computing time and solution quality.

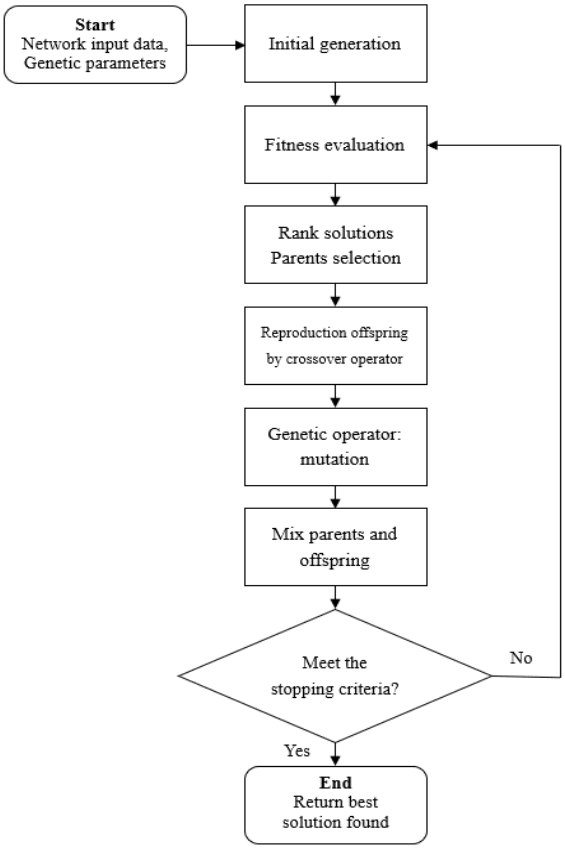

Figure 6. Flowchart of GA

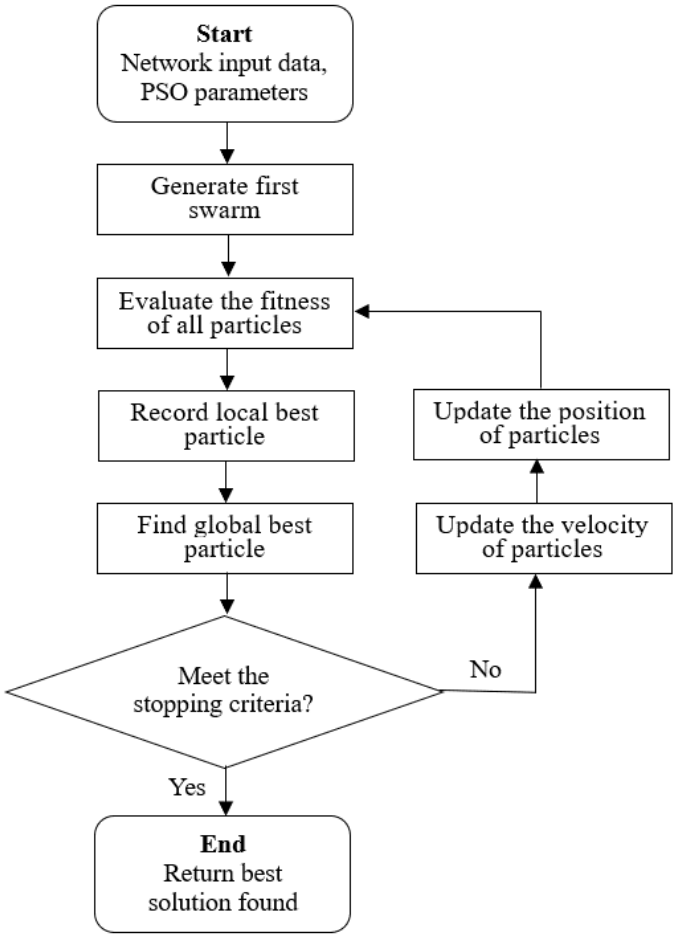

Figure 7. Flowchart of PSO

Chapter 4: Illustrative examples and empirical analysis

4.1 Network Instance and Simulation Disruption

To empirically evaluate the recovery trajectories based on optimizing TRT, SRT, and CRTd and, subsequently, two optimization algorithms (GA and PSO), we generate network instances using a random geometric graph algorithm. The edges of the network are non-directional and capacitated. The geometric graph algorithm generates the network by giving the number of nodes and edges, n and m, respectively, and ensures no disconnected vertices exist. Each edge is then randomly assigned capacity and restoration time. For this study, we simulate four networks of different size and complexity as depicted in Figure 8. Fig. 8 (a) depicts a simple network with 20 nodes and 30 edges. Another simple network, which includes 30 nodes is shown in Fig. 8 (b). Fig. 8 (c) and (d) portray complex networks which contains 40 nodes and 60 edges. The simulated disruption affects the capacities of edges. This provides a simplistic approach to simulating disasters such as an earthquake. We build a five damage level model inspired by Nicholson et al. (2016) which decreases edge flow by 100%, 80%, 50%, 20%, and 0%, respectively, based on distance from the epicenter. The highest level of disruption occurs for those edges that intersect the circle closest to the epicenter. Any edge that cuts across one of these disruptive circles is set to be damaged, and the loss is defined by the smallest of the concentric circles intersected. Figure 9 depicts the disruption area of network and show the number of damaged edges in each instance. Note that, Fig. 8 (c) and (d) show two networks share the same number of nodes and edges, but the random location of the nodes and the center of disaster create the different situation of damage edges.

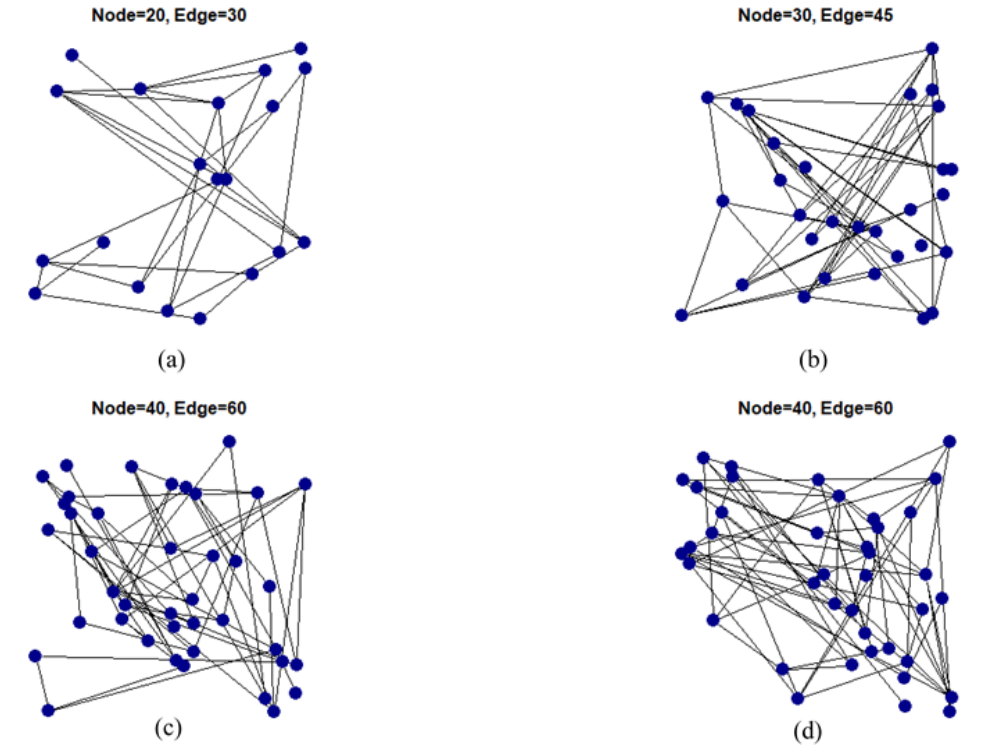

Figure 8. Four Network Design Instances

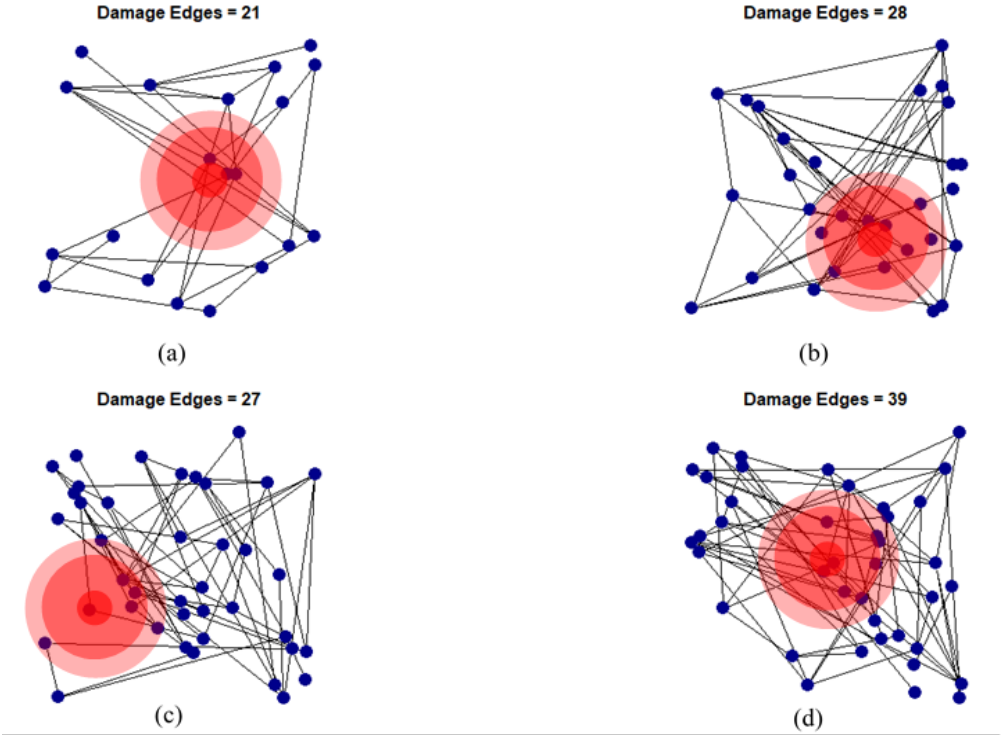

Figure 9. Four Network Instances After Disaster

4.2 Comparison of Measuring Metrics of Network Restoration

In this paper, all models are coded in Sublime Text 2 and run on the laptop with Intel Core i7-7700HQ 2.80 GHz, 16 GB RAM, Windows 64 bits. In this section, we first compare the TRT and SRT metrics. Figure 10 illustrates the network recovery trajectory associated with the optimal schedule found by optimizing TRT and SRT metrics for the four instance networks. In each chart, the horizontal axis denotes the recovery time and the vertical axis represents the performance of network. In each simulation, the number of maximum concurrent repair jobs, N_{max}, is set to three. As mentioned before, the area beneath the recovery trajectory could be considered as a method the measure the recovery schedule. In Figure 10, although the TRT solutions always finish the restoration process earlier than the SRT solutions, the area beneath the trajectory of the optimal TRT schedule is less than the SRT trajectory. This observation agrees with Zhang et al. (2017) and provides evidence that SRT is a better objective than TRT for post-disaster resilience analysis. When we search to optimize TRT alone, the recovery plan focuses on how to complete the job faster, not how to reduce the cumulative catastrophic impact.

SRT and CRTd both consider the shape of the recovery trajectory. However, SRT considers only the time-axis, whereas CRTd considers both the time and performance axes. For a more precise result, we set the $N_{max} = 1$ in following experiments. In this way, we can make sure that the schedules searched by SRT and CRTd have same total recovery time, then we can compare two metrics more

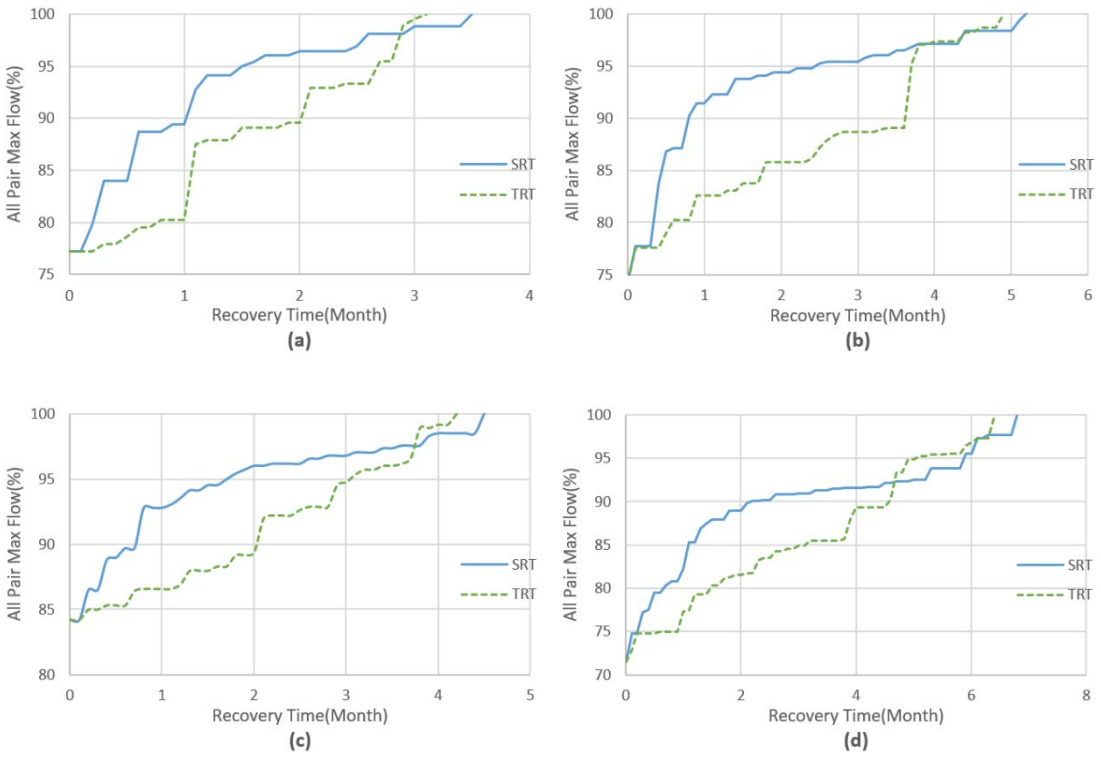

Figure 10. TRT VS. SRT

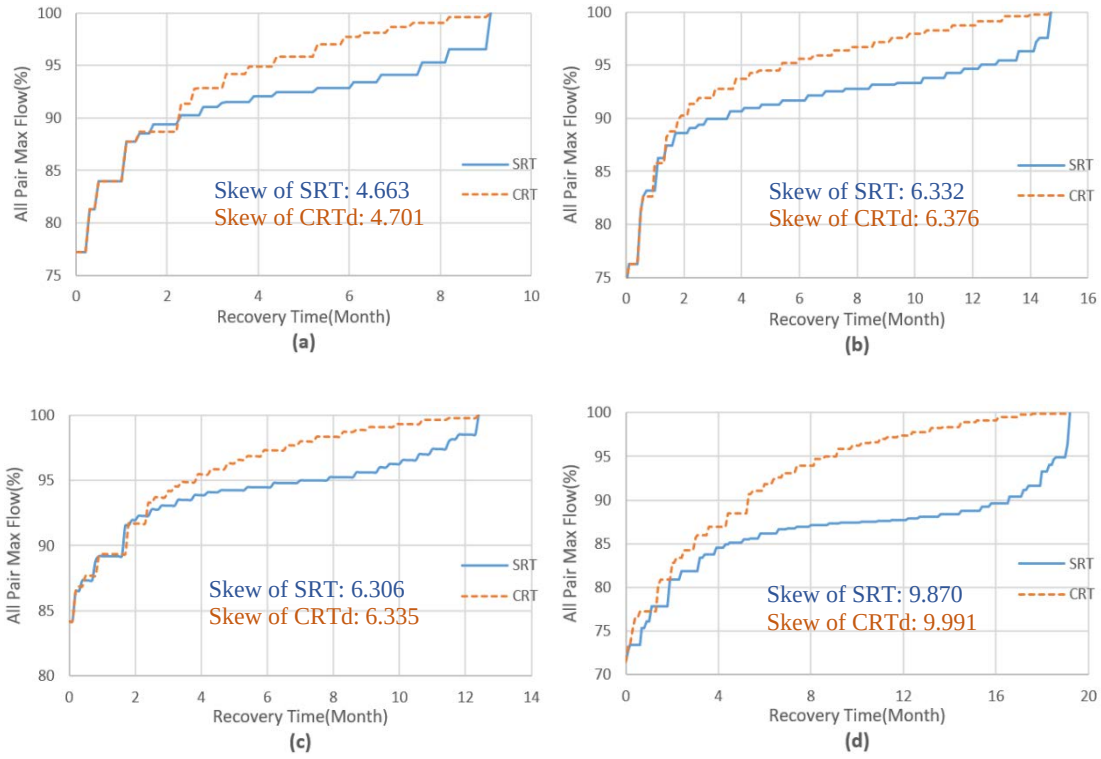

Figure 11. SRT VS. CRTd

clearly. The recovery trajectories determined by attempting to minimize SRT and CRTd for all four random graphs are depicted in Figure 11. Apparently, the SRT and CRTd derived recoveries distinct. The former has slightly improved skew values, however the areas under the restoration curves associated with CRTd are noticeably larger than those associated with the SRT metric. This provides evidence that the additional dimension relating directly to system performance provides a beneficial aspect to the optimization objective.

Moreover, we generate 120 random networks and disruption scenarios and optimize the recovery schedule for each instance. These 120 networks are divided into 12 groups; each group has 10 instances of networks; each network has different location of nodes and randomly location of disaster center. For each of the 120 scenarios, N_{max} is set equal to 3. The average loss values (calculated based on Eq. 11 with theta = 0.01) and the computational time (in seconds) are recorded in Table 2 for the TRT, SRT, and CRTd derived recoveries. In Table 2, node and edge column depict the network size; damage column denotes the range of the damage edges after hazard event; loss shows the mean and standard deviation (SD) of loss values of various scenarios; time depicts the mean and standard deviation of computational time of different scenarios. As shown in Table 2, the computing time of TRT metric is always the shortest one, while the loss value of optimal TRT schedule is apparently higher than the loss value of schedules found by SRT and CRTd. Thus, the TRT is not a reasonable objective for searching the optimal reconstruction plan. Furthermore, the CRTd metric always can find the recovery trajectory with the lowest loss value among three metrics. For instance, in the case of node=30, edge=60, and damage edges range is (40, 50): the average TRT

computing time is around 170(s), while SRT and TRT average computational time are about 1850(s). Also, the average loss value of TRT is 73216; the SRT is 58838; and the lowest average loss value is gained by CRTd metric, which is 45217. Note that, the network size and the number of damage edges both have the influence on the computational time. When the network size is fixed, the calculation time will raise if the number of disrupted edges raise, and vice versa. For example, in the cases of network size is fixed on node=40, edge=80: the average computing time of SRT metric raises from 3195(s) to 6398(s) following the raising of the number of damage edges. One more truth is that when the network size is large, the SRT metric obviously needs longer time than the CRTd for finding the optimal schedule. In the last scenario, SRT average computing time is 21205 seconds while CRTd only needs 7842 seconds. Also, as shown in Table 2, the difference between loss of SRT and CRTd also become more greatly, from 1832 in the first scenario to 31931 in the last scenario.

Table 2. Summary of Three Metrics Comparing (Loss and Time)

Scenario			TRT		SRT		CRTd	
Node	Edge	Damage	Loss	Time$_{(s)}$	Loss	Time$_{(s)}$	Loss	Time$_{(s)}$
20	40	(10, 20)	12804±5734	40±3	8453±648	293±134	6621±332	215±19
20	40	(20, 30)	19254±7284	47±5	13073±6010	518±289	10105±2436	385±122
20	40	(30, 40)	53275±6271	78±5	34172±4129	946±239	30985±1951	848±340
30	60	(20, 30)	27731±11215	124±13	20561±6264	1054±229	17458±4794	992±442
30	60	(30, 40)	56085±29457	150±41	44711±10701	1205±469	35284±6857	1701±566
30	60	(40, 50)	73216±38216	178±36	58838±23838	1804±714	45217±14261	1957±824
40	80	(30, 40)	74863±26023	282±40	48639±25792	3195±955	32532±26185	2533±776
40	80	(40, 50)	96564±48743	314±12	72412±38188	5095±1508	54410±31954	3049±1081
40	80	(50, 60)	140142±34033	324±30	113701±24973	6398±791	72055±19461	3974±1047
50	100	(40, 50)	117655±40550	451±21	90002±18718	8396±965	65796±14915	5794±3944
50	100	(50, 60)	152817±85702	507±53	119167±50144	15355±2132	92504±35133	6816±1140
50	100	(60, 70)	228965±81286	704±82	140205±42162	21205±1502	108274±40159	7842±2663

In Table 3, the R_time column denotes the mean and standard deviation of recovery time (in months); the skew column records the mean and standard deviation value of the skew of recovery trajectory searched by TRT, SRT, and CRTd metrics. Table 3 presents that the longer total recovery time which is searched by SRT and CRTd metrics is at most two months later than the TRT's recovery time. Also, the skew value of the recovery schedule trajectory gained by SRT and CRTd metrics are very close. Compared to the apparent difference in loss value shown in Table 2, the similarity of skew values in Table 3 proves that only considering the SRT is not a valuable method to evaluate the post-disaster reconstruction schedule. For instance, in the case of node=40, edge=80, and damage edges range is (50, 60): the difference between the skew value of SRT and CRTd is only 0.147, but the loss value difference is 41646. All these data demonstrate that, compared with TRT or SRT, the CRTd is the best metric for searching an ideal post-disaster reconstruction schedule.

Table 3. Summary of Three Metrics Comparing (Recovery Time and Skew)

Scenario			TRT		SRT		CRTd	
Node	Edge	Damage	R_Time(m)	Skew	R_Time(m)	Skew	R_Time(m)	Skew
20	40	(10, 20)	8.29±2.12	4.385±0.812	9.84±2.21	4.30±0.739	9.08±2.25	4.331±0.811
20	40	(20, 30)	10.50±2.82	5.360±1.919	11.91±2.52	5.216±1.857	11.73±2.61	5.259±1.649
20	40	(30, 40)	16.94±3.41	8.724±2.784	18.45±4.12	8.353±2.876	18.27±3.60	8.458±2.681
30	60	(20, 30)	14.33±2.36	7.041±1.866	15.94±2.44	6.920±1.853	15.53±2.58	6.962±2.191
30	60	(30, 40)	16.76±3.28	8.135±2.392	18.31±3.12	7.942±2.496	17.92±3.49	8.025±2.243
30	60	(40, 50)	19.75±4.26	10.329±3.138	21.64±3.99	9.744±2.967	21.10±4.41	9.874±2.895
40	80	(30, 40)	17.84±2.60	8.545±2.564	19.94±2.31	8.454±2.628	19.38±2.37	8.486±2.542
40	80	(40, 50)	20.65±3.52	9.735±2.675	22.45±3.83	9.435±2.817	21.51±4.12	9.527±2.474
40	80	(50, 60)	25.03±4.49	12.068±3.016	26.10±4.93	11.626±2.975	25.57±4.63	11.773±2.882
50	100	(40, 50)	21.55±3.76	10.493±2.524	23.16±3.83	10.273±2.479	22.94±3.85	10.354±2.408
50	100	(50, 60)	24.56±4.35	11.683±2.839	25.84±4.29	11.363±2.794	25.48±4.26	11.466±2.768
50	100	(60, 70)	30.62±4.98	14.886±3.074	31.92±5.19	14.365±3.192	31.76±4.87	14.574±3.087

4.3 Comparison of Algorithms

First, we run two optimization models building by GA and PSO algorithms, and both use the CRTd metric on the four instance networks, set the $N_{max} = 1$, and equal population size (number of individuals of each generation) of two models. The optimal recovery schedules obtained by two models are presented in Figure 12. The trajectory searched by PSO is close to the schedule obtained by GA.

Moreover, we run GA and PSO models in the 120 random networks scenarios described in Section 4.2. Additionally, for comparing the GA and PSO, we add a testing GA model which is stopping at the PSO computing time instead of completing the GA procedure. The results are summarized in Table 4; the GA_test column collects the data of the testing model. The loss and time columns in Table 4 also depict the mean and standard deviation of loss value and computing time (in seconds). Table 4 demonstrate that PSO can find a nearly optimal solution by spending much less time than GA. When the network size is small, the testing GA model which stops at the PSO computing time can gain a relative same answer with PSO, but if the network is large, the GA model cannot find an acceptable recovery plan by using PSO running time. For instance, in the first scenario: the average loss value of testing GA and PSO models are 7015 and 6994, both close to the average loss value of GA model. In the last scenario: the loss value of PSO is 137956 which is close to the average loss value of GA (considering the complexity of networks), while the testing GA has a larger loss value, 181382. Under the crisis of post-disaster, time is precious, PSO algorithm can help the decision maker choose a fast near-optimal solution.

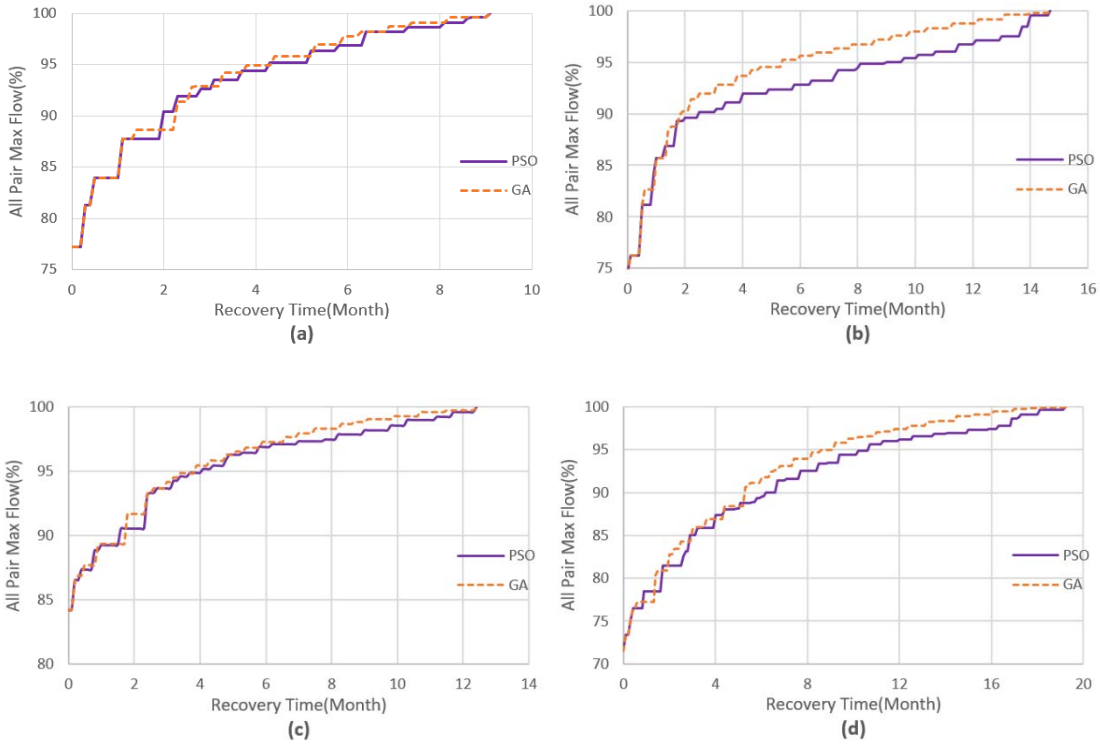

Figure 12. GA VS. PSO

Table 4. Summary of Two Algorithms Comparing

Scenario			GA		PSO		GA_Test	
Node	Edge	Damage	Loss	Time(s)	Loss	Time(s)	Time(s)	Loss
20	40	(10, 20)	6621±332	215±19	6994±854	67±1	7015±393	67±2
20	40	(20, 30)	10105±2436	385±122	10332±2820	110±23	11364±4108	110±23
20	40	(30, 40)	30985±1951	848±340	31075±1891	208±45	35014±1389	209±46
30	60	(20, 30)	17458±4794	992±442	17804±4939	232±46	18229±5761	233±46
30	60	(30, 40)	35284±6857	1701±566	35941±13878	380±177	39742±14102	381±177
30	60	(40, 50)	45217±14261	1957±824	45831±16912	431±211	51865±18949	434±213
40	80	(30, 40)	32532±26185	2533±776	33016±13515	590±68	35532±11903	591±68
40	80	(40, 50)	54410±31954	3049±1081	56211±23262	984±255	58667±20916	988±149
40	80	(50, 60)	72055±19461	3974±1047	76261±12425	1136±239	92739±16866	1141±242
50	100	(40, 50)	65796±14915	5794±3944	68508±21669	1237±811	78634±14896	1242±817
50	100	(50, 60)	92504±35133	6816±1140	98612±31941	1550±127	105806±44175	1553±132
50	100	(60, 70)	108274±40159	8379±2663	137956±40950	2480±253	181382±38349	2491±256

Chapter 5: Conclusion

This paper has presented a new metric to measure the reconstruction schedule of the post-disaster transportation network − centroid of recovery trajectory distance, CRTd. We compared the CRTd with two other metrics, the total recovery time (TRT) and the skew of recovery trajectory (SRT), by two dimensions, the loss value and computational time. The statistical analysis showed that even the TRT metric could find the answer most quickly, but the loss value of TRT is significantly larger than others. The data also proved that as the increasing of network size, the benefit of CRTd metric is more significant. It can detect the better recovery schedule which has less loss value and less computing time than SRT metric. The analysis established that CRTd is a more excellent metric for building the post-disaster transportation network reconstruction strategies optimization model. Moreover, we demonstrated that, compared with the Genetic Algorithm (GA), the Particle swarm optimization (PSO) could generate a nearly optimal solution with less computing time. Another statistical analysis contained the testing GA model, which is stopping at the PSO model computing time, demonstrated that the advantage in computational time of PSO is more obvious when the network is complicated and large. We think our analysis could give the decision maker two options: a time costing but idealized solution searched by GA or a quickly nearly optimized solution gained by PSO.

For the future research, to begin with, the all pairs max flow method is not an ideal method to evaluate the performance of a reality post-disaster transportation network. We desire to develop a network model which could reflect the various levels of the importance of the roads, by considering the role of each road playing in the

functionality of the network. Second, in some discussions, PSO could reach the same optimize solution compared with GA. We wish that we could build a new optimization model by using improved PSO algorithm or more appropriate parameter, and this new PSO model could generate the equally best solution searched by GA.

References

Barker, K., Ramirez-Marquez, J. E., and Rocco, C. M. (2013). Resilience-based network component importance measures. Reliability Engineering and System Safety, 117, 89–97.

Bocchini, P., and Frangopol, D. M. (2012). Restoration of bridge networks after an earthquake: multicriteria intervention optimization. Earthquake Spectra, 28(2), 427–455.

Bruneau, M., Chang, S. E., Eguchi, R T., Lee, G. C., O'Rourke, T. D., Reinhorn, A. M., Shinozuka, M., Tierney, K., Wallace, W.A, and Winterfeldt, D.V. (2003). A framework to quantitatively assess and enhance the seismic resilience of communities. Earthquake Spectra, 19(4), 733–752.

Çağnan, Z., Davidson, R., and Guikema, S. (2004). Post-earthquake restoration modeling of electric power systems. 13th World Conference on Earthquake Engineering, 109, 1–12.

Chang, S. E., and Shinozuka, M. (2004). Measuring improvements in the disaster resilience of communities. Earthquake Spectra, 20(3), 739–755.

Cimellaro, G. P., Reinhorn, A. M., and Bruneau, M. (2006). Quantification of seismic resilience. 8th U.S. National Conference on Earthquake Engineering, 1094.

Cimellaro, G. P., Reinhorn, A. M., and Bruneau, M. (2010a). Framework for analytical quantification of disaster resilience. Engineering Structures, 32(11), 3639–3649.

Cimellaro, G. P., Reinhorn, A. M., and Bruneau, M. (2010b). Seismic resilience of a hospital system. Structure and Infrastructure Engineering, 6(1–2), 127–144.

Cutter, S. L., Burton, C. G., and Emrich, C. T. (2010). Disaster resilience indicators for benchmarking baseline conditions. Journal of Homeland Security and Emergency Management, 7(1).

Dan M. Frangopol and Paolo Bocchini. (2011). Resilience as optimization criterion for the rehabilitation of bridges belonging to a transportation network subject to earthquake, Structures Congress, 2044–2055.

Davidson RA, and Çağnan, Z. (2004). Restoration modeling of lifeline systems. Restoration Modeling of Lifeline Systems.

Edmonds, J., and Karp, R. M. (1972). Theoretical improvements in algorithmic efficiency for network flow problems. Journal of the ACM, 19(2), 248–264.

Filippini, R., and Silva, A. (2014). A modeling framework for the resilience analysis of

networked systems-of-systems based on functional dependencies. Reliability Engineering and System Safety, 125, 82–91.

Ford, L. R.; Fulkerson, D. R. (1956). Maximal flow through a network. Canadian Journal of Mathematics, 8: 399-404.

Franca, P. M., Gendreau, M., Laporte, G., and Muller, F. M. (1996). A tabu search heuristic for the multiprocessor scheduling problem with sequence dependent setup times. International Journal of Production Economics, 43(2–3), 79–89.

Goldberg, D. E. (1989). Genetic algorithms in search, optimization, and machine learning. Reading: Addison-Wesley, 611–616.

Goldberg, A. V., and Tarjan, R. E. (1988). A new approach to the maximum-flow problem. Journal of the ACM, 35(4), 921–940.

Goldberg, A. V, and Tsioutsiouliklis, K. (2001). Cut tree algorithms: an experimental study. Journal of Algorithms, 38(1), 51–83.

Gonçalves, J. F., De Magalhães Mendes, J. J., and Resende, M. G. C. (2005). A hybrid genetic algorithm for the job shop scheduling problem. European Journal of Operational Research, 167(1), 77–95.

Guinet, A. (1993). Scheduling sequence-dependent jobs on identical parallel machines to minimize completion time criteria. International Journal of Production Research, 31(7), 1579–1594.

Hariharan, R., Kavitha, T., Panigrahi, D., and Bhalgat, A. (2007). An Õ(mn) Gomory-Hu tree construction algorithm for unweighted graphs. Proceedings of the Thirty-Ninth Annual ACM Symposium on Theory of Computing, San Diego, 605.

Harris, T. E.; Ross, F. S. (1955). Fundamentals of a method for evaluating rail net capacities. Research Memorandum RM-1573, The RAND Corporation, Santa Monica, California.

John Henry Holland. (1975). Adaptation in natural and artificial systems: an introductory analysis with. Ann Arbor. Univ. of Michigan Press, 1975.

Karamlou, A., and Bocchini, P. (2014). Optimal bridge restoration sequence for resilient transportation networks. Structures Congress 2014, 1, 1437–1447.

Karamlou, A., and Bocchini, P. (2016). Sequencing algorithm with multiple-input genetic operators: Application to disaster resilience. Engineering Structures, 117, 591–602.

Kashan, A. H., and Karimi, B. (2009). A discrete particle swarm optimization algorithm for scheduling parallel machines. Computers and Industrial Engineering, 56(1), 216–223.

Kennedy, R. and Eberhart, J. (1995). Particle swarm optimization. In Proceedings of IEEE International Conference on Neural Networks IV, 1000.

Mattsson, L. G., and Jenelius, E. (2015). Vulnerability and resilience of transport systems - A discussion of recent research. Transportation Research Part A: Policy and Practice, 81, 16–34.

Miles, S. B., and Chang, S. E. (2004). Foundations for modeling community recovery from earthquake disasters. 13th World Conference on Earthquake Engineering, 5, 13.

Nan, C., and Sansavini, G. (2017). A quantitative method for assessing resilience of interdependent infrastructures. Reliability Engineering and System Safety, 157, 35–53.

Nicholson, C. D., Barker, K., and Ramirez-Marquez, J. E. (2016). Flow-based vulnerability measures for network component importance: Experimentation with preparedness planning. Reliability Engineering and System Safety, 145, 62–73.

Odan, F. K., Ribeiro Reis, L. F., and Kapelan, Z. (2015). Real-time multiobjective optimization of operation of water supply systems. Journal of Water Resources Planning and Management, 141(9), 4015011.

R. E. Gomory and T. C. Hu. (1961). Multi-terminal network flows. Society for Industrial and Applied Mathematics, 9(4), 551–570.

Raj, R., Wang, J. W., Nayak, A., Tiwari, M. K., Han, B., Liu, C. L., and Zhang, W. J. (2015). Measuring the resilience of supply chain systems using a survival model. IEEE Systems Journal, 9(2), 377–381.

Schrijver, A. (2002). On the history of the transportation and maximum flow problems. Mathematical Programming, Series B, 91(3), 437–445.

Serhiy Y. Ponomarov and Mary C. Holcomb. (2009). Understanding the concept of supply chain resilience. Int J Logistics Management, 20(1), 124-143

Shinozuka, M., Chang, S. E., Cheng, T., Feng, M., O'Rourke, T. D., Saadeghvaziri, M. A., Dong, X., Jin, X., Wang, Y., Shi, P. (2003). Resilience of integrated power and water systems. Seismic Evaluation and Retrofit of Lifeline Systems, 65–86.

Shinozuka, M., Member, H., Member, A., Lee, J., and Naganuma, T. (2000). Statistical analysis of fragility curves. Journal of Engineering Mechanics, 126(December), 1224–1231.

Sterbenz, J. P. G., Çetinkaya, E. K., Hameed, M. A., Jabbar, A., Qian, S., and Rohrer, J. P. (2013). Evaluation of network resilience, survivability, and disruption tolerance: Analysis, tossspology generation, simulation, and experimentation: Invited paper. Telecommunication Systems, 52(2), 705-36

Tamvakis, P., and Xenidis, Y. (2013). Comparative evaluation of resilience quantification methods for infrastructure systems. Procedia - Social and Behavioral Sciences, 74, 339–348.

UNISDR (2011) Global Assessment Report on Disaster Risk Reduction. United Nations International Strategy for Disaster Reduction, Geneva, Switzerland.

Wang, D., and Ip, W. H. (2009). Evaluation and analysis of logistic network resilience with application to aircraft servicing. IEEE Systems Journal, 3(2), 166–173.

Wang, K.P., Huang, L., Zhou, C.G., Pang, W. (2003) Particle swarm optimization for traveling salesman problem. International Conference on Machine Learning and Cybernetics, Xi'an, 2-5 November, 1583-1585.

Wang, X. (2015). Towards resilience analysis : An efficient way to evaluate network performance. (Unpublished master's thesis), University of Oklahoma, Norman, OK

Weng, M. X., Lu, J., and Ren, H. (2001). Unrelated parallel machine scheduling with setup consideration and a total weighted completion time objective. International Journal of Production Economics, 70(3), 215–226.

Xu, N., Guikema, S. D., Davidson, R. A., Nozick, L. K., Çağnan, Z., and Vaziri, K. (2006). Optimizing scheduling of post-earthquake electric power restoration tasks. International Association for Earthquake Engineering, 44(August 2006), 657–675.

Zhang, C., Xu, B., Li, Y., and Fu, G. (2017). Exploring the relationships among reliability, resilience, and vulnerability of water supply using many-objective analysis. Journal of Water Resources Planning and Management, 143(8), 4017044.

Zhang, W., and Wang, N. (2016). Resilience-based risk mitigation for road networks. Structural Safety, 62, 57–65.

Zhang, W., Wang, N., and Nicholson, C. (2017). Resilience-based post-disaster recovery strategies for road-bridge networks. Structure and Infrastructure Engineering, 13(11), 1404–1413.

Zhang, X., and Miller-Hooks, E. (2015). Scheduling short-term recovery activities to maximize transportation network resilience. Journal of Computing in Civil Engineering, 29(6), 4014087.